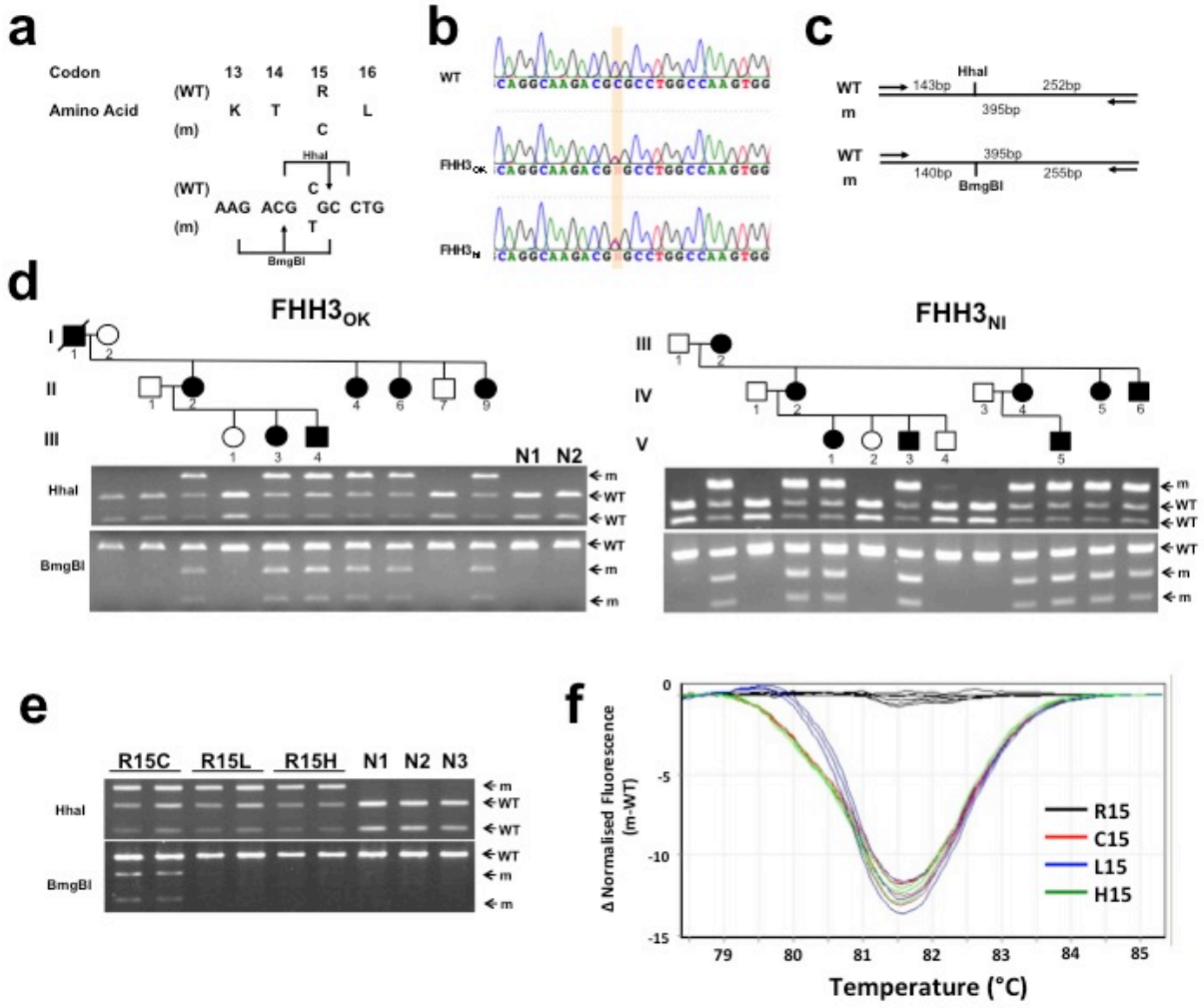


**Supplementary Figure 1. *AP2S1* mutations in FHH3.**

**a**, Exome sequencing revealed a C to T transition, predicting a Arg15Cys (R15C) mutation with loss of the wild-type (WT) *Hha*I (GCG/C) site and gain of a *Bmg*BI (GAC/GTG) site. **b**, Confirmation of mutation by dideoxynucleotide sequence analysis in an affected individual from each of the $FHH3_{OK}$ and $FHH_{NI}$ kindreds[6,7] and its absence in an unrelated normocalcemic (wild-type, WT) individual. **c**, *Hha*I and *Bmg*BI restriction map showing WT and mutant (m) PCR products following digestion. **d**, Co-segregation of *AP2S1* mutation (Arg15Cys) in the unrelated $FHH3_{OK}$ and $FHH3_{NI}$ kindreds with individuals identified using numbers previously reported[6,7]. The family trees are drawn so

that each individual is represented above his/her restriction fragments. All the affected individuals are heterozygous for WT and m alleles, whereas all the unaffected individuals are homozygous for WT alleles, consistent with the autosomal dominant inheritance of FHH3[5-7]. Male (square), female (circle), unaffected (open symbols), affected (filled symbols), and N (unrelated normals). **e,** Detection of Arg15Cys, Arg15His (R15H), and Arg15Leu (R15L) AP2S1 mutations by *Hha*I and *Bmg*BI restriction endonuclease analysis. The Arg15Leu and Arg15His *AP2S1* mutations resulted in only loss of the *Hha*I site. Two patients with each of the three *AP2S1* mutations are shown. These variants were not present in 110 alleles from 55 unrelated normocalcemic individuals (N1 to N3 shown) nor in ~5400 exomes (National Heart, Lung and Blood Institute Exome Sequencing Project), thereby indicating that these abnormalities are likely mutations of *AP2S1* and not polymorphic variants. **f,** Detection of AP2S1 Arg15 mutations by high-resolution melt curve analysis. The *AP2S1* mutant PCR products, which formed heteroduplexes of wild-type (WT) and mutant (m) alleles, melt at lower temperatures (79-80°C) than the homoduplexes of WT *AP2S1* PCR products (>81°C ), thereby facilitating their detection.

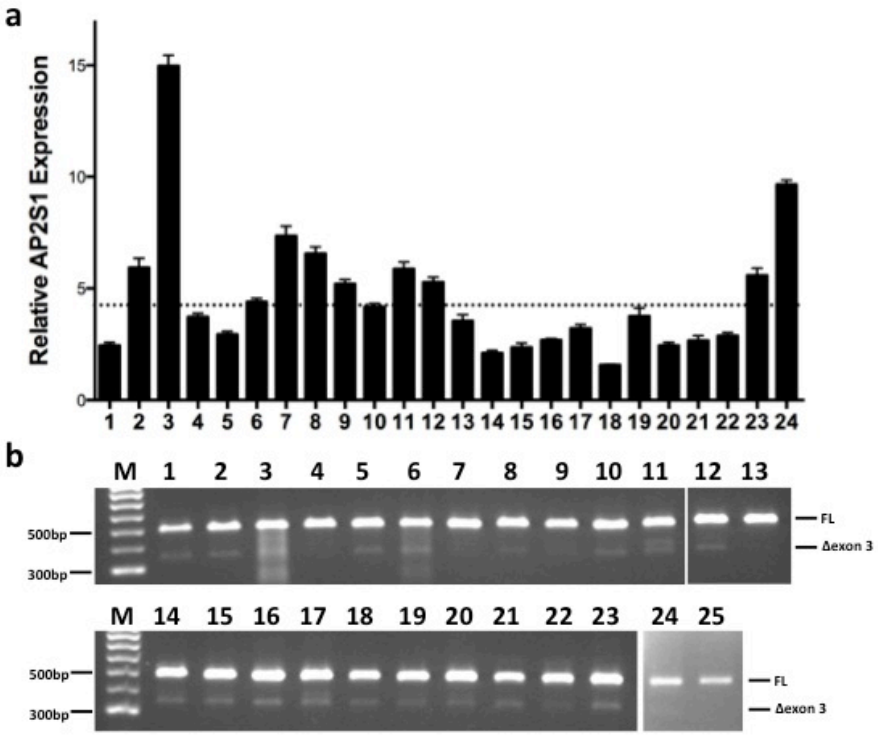


**Supplementary Figure 2. *AP2S1* expression analysis.**

a. Quantitative RT-PCR analysis of AP2S1 expression using total RNA derived from human: 1. Adipose; 2. Bladder; 3. Brain; 4. Cervix; 5. Colon; 6. Esophagus; 7. Heart; 8. Kidney; 9. Liver; 10. Lung; 11; Ovary; 12. Placenta; 13. Prostate; 14. Skeletal Muscle; 15. Smooth Muscle; 16. Spleen; 17. Testis; 18. Thymus; 19; Thyroid; 20. Trachea; 21-23. Parathyroid adenomas; 24. HEK293; 25. CaSR stably-transfected HEK293. The mean relative level of AP2S1 expression is indicated by a dotted line. AP2S1 is ubiquitously expressed and its expression in kidney, parathyroids and HEK293 cells is similar to that in other tissues, except brain, and approximates to that of the mean relative level of AP2S1 expression. b. RT-PCR analysis of AP2S1 alternative splicing in human tissues. The full-length (FL) transcript is the predominant form and the isoform lacking exon 3 (**Δ**exon 3) comprises <5% of the total AP2S1 transcript. The full-length transcript is ubiquitously expressed and the **Δ**exon 3 is expressed in multiple tissues.

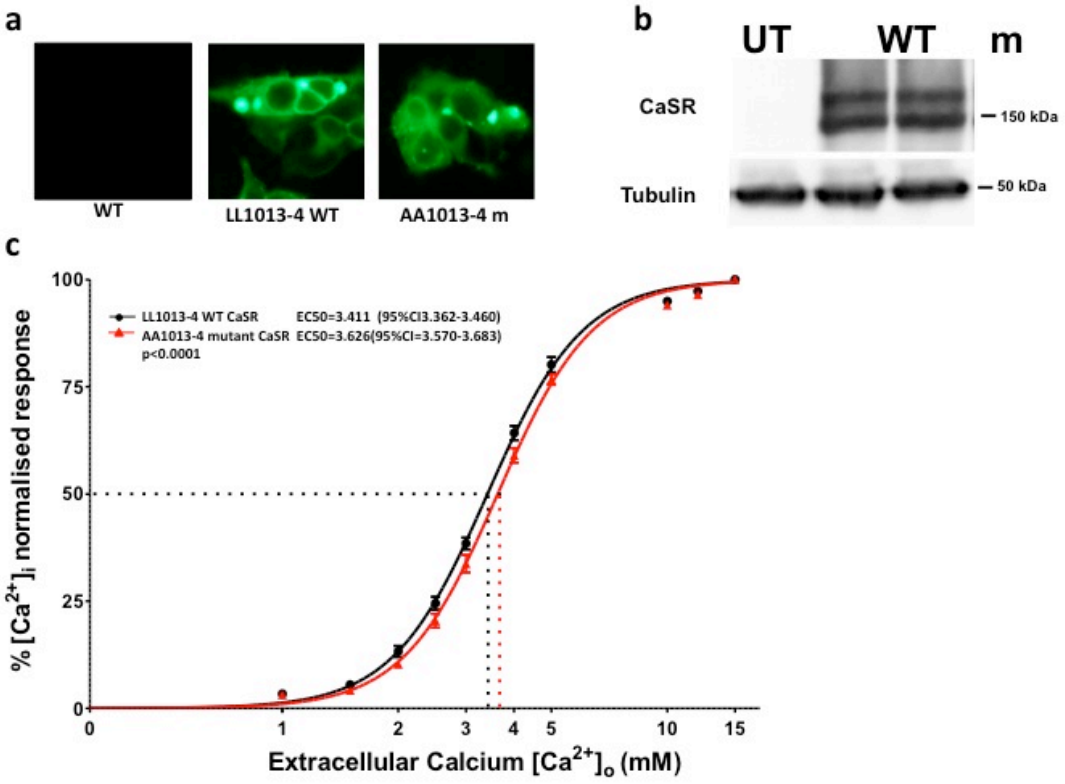


**Supplementary Figure 3. Functional expression in HEK293 cells of wild-type (WT) and mutant (m) CaSRs.**

HEK293 cells were transiently transfected with WT (LL1013-4) or mutant (m)(AA1013-4) CaSR-EGFP constructs. **a**, Fluorescence microscopy confirmed successful transfection. CaSR-EGFP expression is observed at the cell-surface and in intracellular structures but not the nucleus. UT-untransfected cells. **b**, Western blot analysis of total cell protein extracts from the HEK293 cells confirmed expression of EGFP-tagged CaSRs which was not present in UT cells. **c**, Single, live cells loaded with indo-1-acetoxymethylester, emitting fluorescence at 525nm, and hence containing transfected CaSR were selected by fluorescence-activated cell sorting, and the $[Ca^{2+}]_o$-evoked increases in $[Ca^{2+}]_i$ measured. The increments in $[Ca^{2+}]_o$ from 0 to 15mM are shown on the x-axis and the $[Ca^{2+}]_i$ response, which was measured as a percentage of the maximum normalized response, is shown on the y-axis (mean±SEM, n=8). The $EC_{50}$ of the mutant CaSR was significantly

higher than that of the wild-type (mutant $EC_{50}$=3.63mM (95%CI=3.57-3.63mM) versus wild-type $EC_{50}$=3.41 (95%CI=3.36-3.46) p<0.0001), thereby indicating that removal of the CaSR dileucine motif resulted in a loss-of-function of the mutant CaSR.

**Supplementary Table 1. *AP2S1* primer sequences used for reverse-transcriptase PCR (RT-PCR) and genomic amplification**

| Primer | Sequence |
|---|---|
| RT-PCR | |
| RT-F (c.83-102 in exon1) | 5'-GAAGTCCGCTCTAGCTCTGG-3' |
| RT-R (c.561-580 in exon 6) | 5'-GTTTCAGCACCTTCGTCGG-3' |
| Genomic DNA PCR and Sequencing | |
| Exon 1 Forward | 5'-CTGGTTCTTCAGCATCTCG-3' |
| Exon 1 Reverse | 5'-CAGAGAAGGGACTTGTCAGC-3' |
| Exon 2 Forward | 5'-AGCCCTATCTCCCCTCTGG-3' |
| Exon 2 Reverse | 5'-GAAGCAAGCAAGCTCAAAGC-3' |
| Exon 3 Forward | 5'-GAGTGAAGGAGTGAATGTTTTGG-3' |
| Exon 3 Reverse | 5'-AAGAAATGGAGAGGGAGAGTCC-3' |
| Exon 4 Forward | 5'-AGGCTGGTCTTGCACTCCTA-3' |
| Exon 4 Reverse | 5'-AGCTGGGACACAGACCTCAG-3' |
| Exon 5 Forward | 5'-ATCAGAGCCCCAGCTTCC-3' |
| Exon 5 Reverse | 5'-GAAGGACTGCTGGGTTGG -3' |

**Supplementary Note : Clinical Data**

The two previously reported FHH3 kindreds were ascertained, and these consisted of 33 affected and 22 unaffected members[5,7]. In addition, 50 hypercalcemic patients who have been previously reported to not have CaSR mutations, together with 55 unrelated normocalcemic individuals were ascertained9. Serum biochemical analysis was undertaken using previously described methods[5,7,9].